Kinetics and Comparative Reactivity of Human Class I and Class IIb Histone Deacetylases

Brian E. Schultz,* Shawn Misialek, Jiansheng Wu, Jie Tang, Marion T. Conn, Ram Tahilramani, and Lance Wong

Celera, 180 Kimball Way, South San Francisco, California 94080

Received March 19, 2004; Revised Manuscript Received June 24, 2004

ABSTRACT: Histone deacetylase (HDAC) enzymes modulate gene expression through the deacetylation of acetylated lysine residues on histone proteins. They operate in biological systems as part of multiprotein corepressor complexes. To understand the reactivity of isolated HDACs and the contribution of cofactor binding to reactivity, the reaction kinetics of isolated, recombinant human HDACs 1, 2, 3, 6, 8, and 10 were measured using a novel, continuous protease-coupled enzyme assay. Values of k_{cat} and k_{cat}/K_m and the pH dependence of these values were determined for the reactions of each isozyme with acetyl-Gly-Ala-(N^{ϵ}-acetyl-Lys)-AMC. Values of k_{cat} spanned the range of 0.006−2.8 s^{-1}, and k_{cat}/K_m values ranged from 60 to 110000 M^{-1} s^{-1}. The pH profiles for both k_{cat} and k_{cat}/K_m were bell-shaped for all of the HDAC isozymes, with pH optima at approximately pH 8. Values of K_i for the inhibitor trichostatin A were determined for each isozyme. The inhibition constants were generally similar for all HDAC isozymes, except that the value for HDAC8 was significantly higher than that for the other isozymes. The reaction of HDAC8 with an alternative substrate was performed to assess the steric requirements of the HDAC8 active site, and the effect of phosphorylation on HDAC1 activity was examined. The results are discussed in terms of the biological roles of the HDAC enzymes and the proposed reaction mechanism of acetyllysine hydrolysis by these enzymes.

Covalent modification of histone proteins through acetylation and deacetylation is an important determinant of chromatin structure and a regulator of gene expression. Acetylation of histone proteins occurs on lysine residues near the N-termini of these proteins. In conjunction with other modifications of histone proteins and DNA, the acetylation state of histones determines whether the chromatin is in a condensed, transcriptionally silent state or in a form more accessible to the transcription machinery of the cell. In general, hyperacetylation of histone proteins is associated with transcriptional activation of genes. The steady-state histone acetylation level arises from the opposing action of histone acetyltransferase (HAT)[1] and histone deacetylase (HDAC) enzymes. Histone acetylation and the biology of HAT enzymes have been reviewed elsewhere (*1*).

Histone deacetylases have been grouped into three classes. Class I and class II histone deacetylases (HDACs) are zinc-containing hydrolase enzymes. To date, 11 mammalian HDAC genes have been described (*2*, *3*). The division of the proteins into classes I and II is based on protein size, sequence similarity, and organization of the protein domains. Members of class I are related to the yeast RPD3 gene product; this class includes HDAC1, HDAC2, HDAC3, HDAC8, and HDAC11. Class II contains HDAC4, HDAC5, HDAC6, HDAC7, HDAC9, and HDAC10, homologues of the yeast HDA1 protein. Class II HDACs have been further subdivided into classes IIa (HDACs 4, 5, 7, and 9) and IIb (HDACs 6 and 10) (*3*). The third class of deacetylases consists of the members of the Sir2 family of enzymes (*4*). These enzymes have histone deacetylase activity but are structurally and evolutionarily unrelated to the class I and class II proteins. They are NAD-dependent and do not contain a catalytic zinc site as do the class I and class II deacetylases. In this work we will use the term HDAC to refer only to the class I and class II enzymes.

In the cell, HDAC proteins are recruited as part of multicomponent repressor complexes (*5*−*7*). Several HDAC-containing complexes have been characterized, including the N-CoR/SMRT, Sin3, NuRD, and CoREST complexes. Within these complexes, HDACs 1 and 2 typically interact with the mSin3, Mi-2, or CoREST proteins. HDAC3 and the class IIa HDACs have been shown to interact with SMRT and the related N-CoR protein. A large number of transcription factors have been shown to bind to one of the corepressor complexes as a means of regulating transcription; these factors have been reviewed elsewhere (*7*). Interaction partners for the other HDAC isozymes are also being investigated (*8*−*10*). The recruitment of HDACs by DNA-

* Corresponding author. Phone: (650) 866-6536. Fax: (650) 866-6653. E-mail: brian.schultz@celera.com.

[1] Abbreviations: AMC, 7-amino-4-methylcoumarin; CoREST, corepressor for RE1 silencing transcription factor; DNP-Dap, 3-(2,4-dinitrophenyl)-L-2,3-diaminopropionic acid; FRET, fluorescence resonance energy transfer; HAT, histone acetyltransferase; HDAC, histone deacetylase; HOBt, 1-hydroxybenzotriazole; N-CoR, nuclear receptor corepressor; NMM, *N*-methylmorpholine; NTA, nitrilotriacetic acid; NuRD, nucleosome remodeling and histone deacetylation; PyBOP, benzotriazol-1-yloxytripyrrolidinophosphonium hexafluorophosphate; SMRT, silencing mediator for retinoid and thyroid hormone receptors; TCEP, tris(2-carboxyethyl)phosphine hydrochloride; TPCK, tosyl-L-phenylalanine chloromethyl ketone; TSA, trichostatin A; Z, benzyloxycarbonyl.

10.1021/bi0494471 CCC: $27.50
Published on Web 08/06/2004

binding proteins allows histone deacetylation to be directed toward specific regions of the chromatin in order to promote targeted transcriptional repression.

HDAC proteins are promising therapeutic targets on account of their involvement in regulating genes involved in cell cycle progression and control (*11*). Inhibition of HDACs has been shown to upregulate genes, including $p21^{WAF/CIP1}$, p27, p53, and cyclin E, and to downregulate genes such as cyclin A and cyclin D. Growth inhibition in several lines of cancer cells has been observed upon treatment with HDAC inhibitors, and in vivo studies have shown that some of these inhibitors are efficacious in slowing tumor growth.

The biological activity of each of the HDAC isozymes is determined by a combination of the intrinsic activity of the enzyme and the effects of cofactor binding on reactivity and substrate recognition. As a means of understanding the intrinsic reactivity of isolated HDAC enzymes, the role of cofactors in modulating this activity, and how differences in enzyme kinetics among the isozymes help to define the biological roles of the HDACs, we have performed quantitative kinetic studies on 6 of the 11 HDAC isozymes. Values of k_{cat} and K_m and the pH dependencies of these parameters were determined for the reaction of HDACs 1, 2, 3, 6, 8, and 10 with a tripeptide substrate, and inhibition constants were determined for trichostatin A, a representative HDAC inhibitor. In addition to providing insight into the mechanism of acetyllysine hydrolysis by the HDAC isozymes, this work provides a basis for exploring substrate specificities of the HDAC enzymes and the kinetics of deacetylation catalyzed by intact HDAC-containing corepressor complexes.

EXPERIMENTAL PROCEDURES

Preparation of HDAC Proteins. The HDAC1 gene was cloned from a human uterine cDNA library and subcloned in frame with a C-terminal FLAG epitope tag as described (*12*). The HDAC1-FLAG coding region was subcloned into baculovirus transfer vector pAcSG2. Recombinant virus was generated using Baculogold DNA according to the manufacturer's instructions (Pharmingen). Sf9 cells were grown in suspension culture and infected with recombinant virus (MOI = 1). Cells were harvested 72 h postinfection and centrifuged at 10000*g* to pellet. Lysates were prepared by sonication of the cell paste in an equal volume of 25 mM Tris, 150 mM NaCl, and 0.5% Nonidet P40 detergent supplemented with EDTA-free protease inhibitor (Roche) according to the manufacturer's instructions. The suspension was diluted 3-fold with 25 mM Tris, 25 mM NaCl, 0.5% Triton X-100, and 10% glycerol, pH 7.4 (buffer A), and centrifuged for 60 min at 16000*g*. The supernatant was loaded onto a Q-Sepharose FF column (Pharmacia) equilibrated with buffer A. Enzyme was eluted using a gradient composed of buffer A and 25 mM Tris, 1 M NaCl, 0.5% Triton X-100, and 10% glycerol, pH 7.4 (buffer B). Buffer B was varied from 0% to 100% over 15 column volumes. Fractions containing HDAC1 were pooled and subjected to dialysis against 25 mM Tris, 150 mM NaCl, and 10% glycerol, pH 7.8. The sample was adsorbed onto anti-FLAG gel (Sigma) and eluted with 20 mg/mL FLAG peptide in 25 mM Tris, 200 mM NaCl, and 10% glycerol, pH 7.1. The protein was dialyzed against 25 mM Tris, 200 mM NaCl, and 10% glycerol, pH 7.1, distributed into storage tubes, and stored at −80 °C.

HDAC2 was cloned from a human placenta cDNA library and subcloned with a C-terminal FLAG tag into the pENTR Gateway vector (Invitrogen). The HDAC2-FLAG coding region was transferred into pDEST8 vector and transfected into DH10Bac cells to generate recombinant bacmid according to the manufacturer's instructions (Invitrogen's Bac-to-Bac). Sf9 cells were grown in suspension culture and infected with recombinant virus at MOI = 5 for 72 h. Cell paste was suspended in a lysis buffer consisting of 50 mM Tris, 150 mM NaCl, 1 mM EDTA, and 1% Triton X-100, pH 7.4, supplemented with protease inhibitor cocktail (Roche) and incubated on ice for 30 min. The mixture was centrifuged at 23700*g* for 15 min at 4 °C. The supernatant was incubated for 2 h with anti-FLAG M2 agarose (Sigma), and the mixture was transferred to a chromatography column. The resin was washed sequentially with 50 mM Tris, 150 mM NaCl, and 0.05% Triton X-100, pH 7.4; 50 mM Tris, 1 M NaCl, and 0.05% Triton X-100, pH 7.4; and 50 mM Tris and 150 mM NaCl, pH 7.4 (TBS). The protein was eluted with 100 μg/mL FLAG peptide in TBS. Fractions containing HDAC2 were pooled to yield protein at 90−95% purity based on gel staining. Aliquots of the protein were transferred to storage tubes and stored at −80 °C.

HDAC3 was cloned from a human colon cDNA library into the pENTR Gateway vector. To generate recombinant virus, the HDAC3-FLAG coding region was transferred into the pDEST10 vector, which added a 6×His tag at the N-terminus, and transfected into DH10Bac cells. A fragment of the mouse SMRT gene coding residues 395−489 was cloned into baculovirus in frame with a C-terminal FLAG tag as described in the literature (*13*). Sf9 cells were grown in suspension culture and co-infected with the two virus constructs at MOI = 2 for 72 h. Cell lysis and protein purification were performed as described for HDAC2. The protein was eluted with 150 μg/mL FLAG peptide in TBS. An HDAC3:SMRT ratio of 1:1 was determined using HPLC. Gel filtration chromatography was used to verify that the complex existed as an intact heterodimer and did not aggregate further. Fractions containing the HDAC3/SMRT heterodimer were pooled, transferred to storage tubes, and stored at −80 °C.

Baculovirus expressing N-terminal 6×His-tagged HDAC8 was used to infect Sf9 cells. The Sf9 cells were grown in suspension culture and infected with virus at MOI = 5 for 72 h. The cell paste was suspended in 50 mM Tris, 200 mM NaCl, and 1 mM TCEP, pH 7.9, supplemented with EDTA-free protease inhibitor mix (Roche), stirred for 20 min at room temperature, and incubated for 40 min at 4 °C. The lysate was centrifuged at 22400*g* for 15 min. The supernatant was recovered and spun for 15 min at 100000*g*. The resulting supernatant was applied to a Ni-NTA column, washed with 20 mM Tris, 1 M NaCl, 30 mM imidazole, and 250 μM TCEP, pH 8.0, and eluted with 20 mM Tris, 0.5 M NaCl, 250 mM imidazole, and 250 μM TCEP, pH 7.0. The eluent was concentrated using a YM-10 ultrafiltration membrane (Millipore) and applied to a Sephacryl S200 column (Pharmacia). The protein was eluted with 25 mM Tris, 150 mM Tris-HCl, and 250 μM TCEP, pH 7.6. Fractions containing the isolated protein were pooled, transferred to storage tubes, and stored at −80 °C.

HDAC6 and HDAC10 were cloned from a human liver cDNA library and subcloned with a C-terminal FLAG tag into the pENTR Gateway vector. To generate recombinant virus, the HDAC-FLAG coding region was transferred into pDEST10 vector, which added a 6×His tag at the N-terminus. The final destination vector was transfected into DH10Bac cells to generate bacmid DNA. Sf9 cells were grown in suspension culture and infected with recombinant virus at MOI = 2 for 72 h. Cell lysis and protein purification were performed as described for HDAC2. The protein was eluted with 150 μg/mL FLAG peptide in TBS. Fractions containing the HDAC protein were pooled, transferred to storage tubes, and stored at −80 °C.

Peptide Synthesis. For the synthesis of acetyl-Gly-Ala-(*N*$^{\epsilon}$-acetyl-Lys)-AMC (**1**), 445 mg (1 mmol) of *tert*-Boc-(*N*$^{\epsilon}$-acetyl-Lys)-AMC (Bachem) was added to 4 M HCl in dioxane to yield H-(*N*$^{\epsilon}$-acetyl-Lys)-AMC as a white solid. The solid was dissolved in 5 mL of DMF and reacted with 188 mg (1 mmol) of Ac-Gly-Ala-OH in the presence of 520 mg (1 mmol) of PyBOP, 135 mg (1 mmol) of HOBt, and 0.296 mL (2 mmol) of NMM. After 1 h of stirring additional amounts of PyBOP (260 mg), HOBt (70 mg), and NMM (0.146 mL) were added. The reaction mixture was stirred for an additional 4 h, after which time the product was isolated in nearly quantitative yield. The purity was >95% as determined by HPLC. The MH^+ peak was observed in the mass spectrum at $m/z = 516$. Acetyl-Gly-Ala-Lys-AMC (**2**) was synthesized in an equivalent fashion, using Ac-Gly-Ala-OH and H-Lys(Z)-AMC (Bachem) as starting materials. After the coupling reaction was complete, the Z group was removed by hydrogenation in a Parr apparatus using 10% Pd on carbon in a solution of ethanol. The final product was purified to >95% purity using preparative HPLC and was further characterized using LC-MS (MH^+ $m/z = 474$) and NMR.

Other Materials. The peptide (2-aminobenzoyl)-Gly-Ala-(*N*$^{\epsilon}$-acetyllysyl)-Ala-Ala-(DNP-Dap)-NH_2 (**3**) was purchased from California Peptide Research, Inc. (Napa, CA). Trichostatin A (TSA) was purchased from Sigma and used as received. TPCK-treated bovine pancreatic trypsin was purchased from Sigma. Active site titrations of trypsin were performed using the MUGB method (*14*).

General Reaction Conditions. Reactions of the HDAC enzymes with **1** were performed at 22 °C in 96-well assay plates with a reaction volume of 100 μL. Unless otherwise specified, reactions were run in the presence of 50 nM trypsin in 50 mM HEPES, 100 mM KCl, 0.001% Tween-20, and 5% DMSO, pH 7.4, supplemented with 0% (HDAC1), 0.01% (HDACs 2, 3, 8, 10), or 0.05% (HDAC6) bovine serum albumin. The reactions were monitored using Molecular Devices Fmax fluorescence microplate readers, with an excitation wavelength of 355 nm and a detection wavelength of 460 nm. After a 30 min lag phase, the reaction was monitored for 30 min to yield reaction rates. The kinetic traces were linear over this time range.

The reactions of HDAC1 and HDAC8 with **3** were performed as described above, with excitation and detection wavelengths of 320 and 405 nm, respectively. An empirical correction was applied to the data to account for the attenuation of the fluorescence of the aminobenzoyl group with increasing concentrations of **3**.

Active Site Titrations. For each HDAC isozyme, ten-point dose−response curves for TSA inhibition were generated at each of four to six different enzyme concentrations. The enzyme concentration typically varied by a factor of 2 between each dose−response curve. The concentration of **1** was held constant at a value between 20 and 100 μM, depending on the HDAC isozyme. Each dose−response curve was generated using 2-fold serial dilutions of TSA, with a starting concentration between 25 nM and 10 μM, depending on the isozyme. Other conditions were as listed above. The program Scientist (MicroMath) was used to perform a global fit of eq 1 (*15*) to the data, where v_0 is the

$$\frac{v}{v_0} = \frac{\alpha[E]_t - [I]_t - K_i' + \sqrt{(\alpha[E]_t - [I]_t - K_i')^2 + 4\alpha[E]_t K_i'}}{2\alpha[E]_t} \quad (1)$$

rate of the enzyme reaction in the absence of inhibitor, $[E]_t$ and $[I]_t$ are the total concentrations of enzyme and inhibitor, K_i' is the apparent inhibition constant, and α is the fractional activity of the enzyme. The fitting routine utilized the Levenberg−Marquardt algorithm to perform a least-squares fit of two variables, the inhibition constant K_i' and the activity term α.

Enzyme Inhibition. Inhibition of HDAC1 by TSA was performed using 200 pM HDAC1, 50 nM trypsin, 1−80 μM **1**, and TSA concentrations of 0, 0.2, 0.4, 0.6, 0.8, and 1.0 nM in 50 mM HEPES, 100 mM KCl, 0.001% Tween-20, and 5% DMSO, pH 7.4. The data were fit with eq 2 (*15*) using the Scientist program as described above, with K_i' and K_i related by eq 3 for a competitive inhibitor. Least-squares

$$v = \frac{k_{cat}[S]([E]_t - [I]_t - K_i' + \sqrt{([E]_t - [I]_t - K_i')^2 + 4[E]_t K_i'})}{2(K_m + [S])} \quad (2)$$

$$K_i' = K_i(1 + [S]/K_m) \quad (3)$$

fitting was used to obtain values of k_{cat}, K_i, and K_m. K_i values for TSA against the other HDAC isozymes were determined as part of the active site titrations described above.

pH Dependence of Enzyme Activity. Reactions were performed by mixing HDAC enzyme, 50 nM bovine trypsin, and **1** in the concentration range of 1.5−150 μM in 50 mM buffer, 100 mM KCl, 0.001% Tween-20, and 2% DMSO. BSA (0%, 0.01%, or 0.05%) was included as described above. At pH 6, 100 nM trypsin was used because of its decreased activity at low pH. Specific buffers were MES (pH 6, 6.5), HEPES (pH 7, 7.4, 7.5, 8), Tris (pH 7.4, 7.5, 8, 8.5, 9), Bicine (pH 8, 8.5), CAPSO (pH 9, 9.5, 10), and CAPS (pH 10, 10.5). Values of k_{cat}, K_m, and k_{cat}/K_m were obtained at each pH value by fitting eq 4 to the data. When an enzyme could not be saturated with substrate because of limited solubility, k_{cat}/K_m was determined by fitting eq 5 to the data. No significant inhibition of the HDAC isozymes was observed with any of the buffers. The pK_a values associated with k_{cat} and k_{cat}/K_m were determined from

nonlinear least-squares fitting of the data with eq 6, where $y = k_{cat}$ or k_{cat}/K_m, A is a normalization constant, and K_1 and K_2 are acid dissociation constants for singly protonated species.

$$v = \frac{k_{cat}[E][S]}{K_m + [S]} \quad (4)$$

$$v = \frac{k_{cat}}{K_m}[E][S] \quad (5)$$

$$y = \frac{A}{1 + [H^+]/K_1 + K_2/[H^+]} \quad (6)$$

Phosphorylation of HDAC1. Phosphorylation of HDAC1 was performed by reacting 30 nM HDAC1 with 1 μL of recombinant human casein kinase II (Calbiochem, 500000 units/mL) in 50 mM HEPES, 100 mM KCl, 10 mM $MgCl_2$, 200 μM ATP, and 0.001% Tween-20, pH 7.4, in a total reaction volume of 100 μL for 2 h. Alkaline phosphatase treatment of HDAC1 was performed by the addition of 1 μL of 0.1 mg/mL placental alkaline phosphatase (Clontech) to 30 nM HDAC1 in 50 mM CAPSO, 100 mM KCl, and 0.001% Tween-20, pH 9.5, in a 100 μL reaction volume. Activity assays of the treated HDAC samples were run with 320 pM HDAC1, 25 μM **1**, and 50 nM trypsin in 50 mM HEPES, 100 mM KCl, 0.001% Tween-20, and 0.25% DMSO, pH 7.4. Gel electrophoresis was performed using an 8% polyacrylamide−Tris/glycine gel. The protein was transferred to a nylon filter, blocked for 1 h with 2% milk, incubated with FLAG antibody in 2% milk for 2 h, and washed three times in TBS. The blot was probed with goat anti-mouse secondary antibody conjugated with alkaline phosphatase (Pierce).

RESULTS

Description of the HDAC Activity Assay. To measure the activity of the HDAC enzymes, we developed a continuous protease-coupled assay analogous to other reported HDAC assays that were implemented in an end point format (*16*, *17*). The assay is diagrammed in Figure 1. The assay relied on the specificity of the proteolytic enzyme trypsin for peptides with a basic amino acid residue in the P1 position. The HDAC substrate acetyl-Gly-Ala-(N^{ϵ}-acetyl-Lys)-AMC (**1**) showed no reaction with trypsin over at least 90 min under conditions of up to 100 nM trypsin and 200 μM **1**, as measured by release of AMC from the peptide. When **1** reacted with an HDAC enzyme, the acetyl group on the lysine residue was cleaved to yield acetyl-Gly-Ala-Lys-AMC (**2**), which reacted readily with trypsin to liberate AMC. The increase in fluorescence at 460 nm arising from the generation of free AMC was used as the measure of HDAC activity. A standard curve of AMC fluorescence was used to convert the measured fluorescence into concentration units.

A representative time course for the reaction of HDAC1 with **1** in the presence of trypsin is shown in Figure 2. A lag phase was observed for this reaction, during which the concentration of **2** rose to its steady-state level. Under the conditions used in our experiments, the lag phase was complete within 30 min. Following the lag phase, the reaction rate was constant for at least 30 min. For all reactions, the

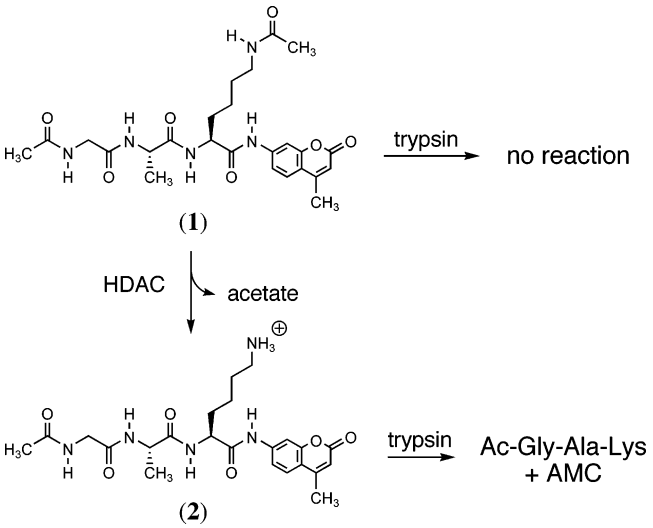

FIGURE 1: Schematic diagram of the HDAC assay. Substrate **1** does not react with trypsin. Following deacetylation of the lysine by an HDAC enzyme, product **2** reacts with trypsin to liberate AMC that is detected by fluorescence spectroscopy.

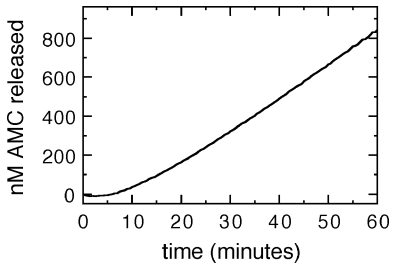

FIGURE 2: Time course of the reaction of HDAC1 with **1** at pH 7.4. The concentrations of HDAC1, trypsin, and **1** were 200 pM, 50 nM, and 25 μM, respectively. Other reaction conditions were as described in the text.

reaction rate was determined from the slope of the progress curve in the interval of 30−60 min.

Compared with other reported HDAC assays that operate in an end point format (*16*−*19*), the continuous, fluorescence-based assay developed for this work provided a more efficient method of obtaining accurate rate data. The rate of AMC release from **2** at steady state was a quantitative measure of HDAC activity, and the reaction rates were determined from a full progress curve rather than from only a few data points. In addition, this assay format allowed for a facile observation of any deviations from linearity in the kinetic progress curves that would indicate substrate depletion or loss of enzyme activity over the course of the reaction.

Kinetic Parameters. Reaction rates were determined for the reactions of the isolated HDACs 1, 2, 6, 8, and 10 with **1**. As an isolated recombinant protein, HDAC3 showed negligible activity, but coexpression of the protein with residues 395−489 of the SMRT protein as described previously (*13*) yielded a highly pure heterodimer with >90% activity. This heterodimer was used in the activity assay with **1**. For brevity we refer to this enzyme complex as HDAC3/SMRT.

Kinetic parameters for the reactions of the HDAC isozymes with **1** are presented in Table 1. For most of the HDACs, measured K_m values were very similar. The exception to this trend was HDAC8, for which the reaction rate was linear with the concentration of **1** to concentrations >200 μM. This

Table 1: Kinetic Parameters and Inhibition Constants for Reactions of HDAC Isozymes with **1**

	HDAC1	HDAC2	HDAC3/SMRT	HDAC6	HDAC8	HDAC10
k_{cat}, s^{-1}	2.8 ± 0.2	2.0 ± 0.2	1.5 ± 0.1	0.7 ± 0.2	nd[a]	0.006 ± 0.002
K_m, μM	25 ± 3	32 ± 4	35 ± 1	18 ± 2	>200	36 ± 3
k_{cat}/K_m, $M^{-1}\,s^{-1}$	110000 ± 15000	62000 ± 10000	43000 ± 3000	39000 ± 12000	60 ± 7	170 ± 60
pK_a (k_{cat})	6.2 ± 0.2	6.5 ± 0.2	7.3 ± 0.1	6.9 ± 0.2	nd	6.4 ± 0.1
	10.5 ± 0.1	9.7 ± 0.2	9.4 ± 0.1	8.3 ± 0.2		10.0 ± 0.1
pK_a (k_{cat}/K_m)	7.0 ± 0.1	7.7 ± 0.1	7.6 ± 0.1	7.4 ± 0.7	7.6 ± 0.1	6.5 ± 0.1
	9.5 ± 0.1	8.5 ± 0.2	9.5 ± 0.1	8.0 ± 0.7	8.9 ± 0.1	9.9 ± 0.1
K_i (TSA), nM	0.23 ± 0.02	0.76 ± 0.05	0.58 ± 0.07	0.99 ± 0.38	130 ± 20[b]	7 ± 2

[a] nd = not determined. [b] Value reported as K_i' rather than K_i.

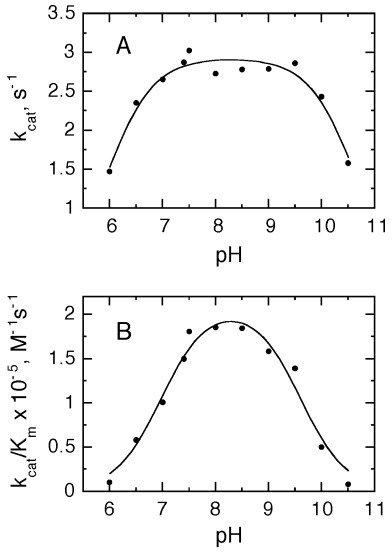

FIGURE 3: pH dependence of the reaction of HDAC1 with **1**. (A) k_{cat} vs pH. (B) k_{cat}/K_m vs pH. The concentration of active HDAC1 was 400 pM. Other reaction conditions were as described in the text.

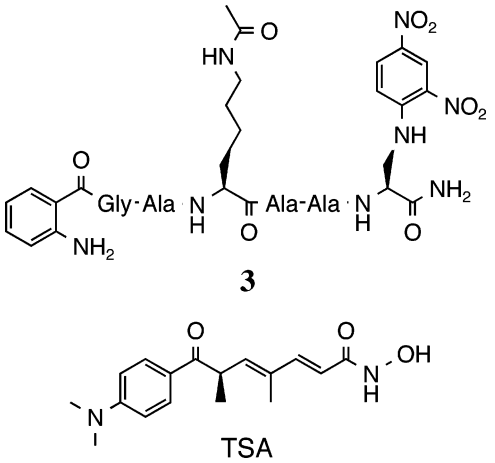

FIGURE 4: Structures of the HDAC substrate (2-aminobenzoyl)-Gly-Ala-(N^{ϵ}-acetyllysyl)-Ala-Ala-(DNP-Dap)-NH_2 (**3**) and the inhibitor trichostatin A.

result is consistent with observations made in an earlier report (*16*). Values of k_{cat} and k_{cat}/K_m for each of the HDAC enzymes were measured as a function of pH. The pH profiles for k_{cat} and k_{cat}/K_m for all isozymes were bell-shaped, with maxima in the range of pH 7.6−8.3. As a representative example, the pH dependence for HDAC1 is shown graphically in Figure 3.

HDAC6 possesses two homologous catalytic domains, both of which were shown to be active and to operate independently (*20*). The two active sites displayed comparable activity in deacetylating histone proteins in vitro. Both of the sites could be inhibited by TSA. Following the discovery that HDAC6 acts as a tubulin deacetylase (*21*, *22*), it was shown that the tubulin deacetylase activity arises from only the C-terminal active site (*23*). In our study, no discrimination was made between the two domains, and the kinetic parameters were reported on the basis of the number of active sites, not the number of protein molecules. In the determinations of the pK_a values associated with k_{cat}/K_m for HDAC6, the two measured pK_a values were routinely separated by less than 0.6 pH unit. As discussed elsewhere, this behavior can arise from cooperative proton binding to the active site residues (*24*). However, in accord with common practice, the pK_a values were reported with a ΔpH of 0.6 unit, the theoretical limit assuming noncooperative proton binding.

Inhibition of the HDAC Enzymes. The reactions of the HDAC isozymes with **1** in the presence of the inhibitor trichostatin A (TSA) were performed to measure the binding constants of this inhibitor, to provide a measurement of the concentration of active enzyme in the reactions, and to assess the differences in the active site structures of the HDAC enzymes. The structure of TSA is shown in Figure 4, and measured K_i values are given in Table 1. For the reactions of the HDAC enzymes with **1** in the presence of TSA, the concentrations of enzyme and inhibitor were generally comparable, and the kinetics were treated using equations for reversible tight-binding inhibition (*15*). This analysis yielded values of both K_i' and the active site concentration of each enzyme. The percent activity for each HDAC isozyme determined from these experiments was used in the calculation of k_{cat} values for each HDAC.

Data for the inhibition of HDAC1 by TSA, along with a global fit of the data, are shown in Figure 5A. A value of 500 pM was determined as the K_i' for TSA. To demonstrate the mode of HDAC1 inhibition by TSA, the reaction rate of HDAC1 with **1** was measured as a function of the concentrations of both **1** and TSA as described above. The data and a global fit with a tight-binding competitive inhibition model (eq 2) are shown in Figure 5B. A K_m value of 23 μM and a K_i value of 230 pM were obtained from the fit. The K_i value is in good agreement with a value of 250 pM derived from the active site titration using $[S]/K_m = 1$. A classical competitive inhibition model and a tight-binding noncompetitive inhibition model both yielded poor fits to the data.

Competitive inhibition was assumed for the other HDAC isozymes. K_i values were calculated using eq 3. For HDAC8, the inhibition constant for TSA was reported as a K_i' value because the K_m value could not be determined. Because [**1**]

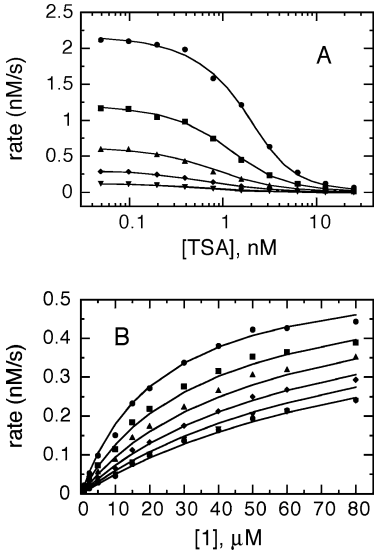

FIGURE 5: (A) Active site titration of HDAC1 with trichostatin A. Concentrations of active HDAC1 were 0.16, 0.32, 0.64, 1.28, and 2.56 nM. (B) Inhibition of HDAC1 by trichostatin A. Rate vs [**1**] plots are shown at TSA concentrations of 0, 200, 400, 600, 800, and 1000 pM.

$\ll K_m$, the true K_i value for TSA should be nearly the same as the K_i' value.

Effect of the AMC Group on Substrate Reactivity. To assess whether the AMC moiety of **1** hindered the binding and turnover of substrate by HDAC8, an alternative substrate was designed with a FRET donor−quencher pair in order to remove any bulky chromophores from the immediate active site. The peptide, (2-aminobenzoyl)-Gly-Ala-(N^{ϵ}-acetyllysyl)-Ala-Ala-(DNP-Dap)-NH_2 (**3**; see Figure 4), was reacted with both HDAC1 and HDAC8 and analyzed as described above. The assay format was identical to that for the reactions of the HDAC enzymes with **1**, except that trypsin cleavage of the deacetylated substrate separated the fluorescent aminobenzoyl group from the fluorescence quencher DNP-Dap to give an increase in fluorescence at 405 nm. The reaction rate of HDAC8 with **3** remained linear with [**3**] at substrate concentrations up to at least 150 μM. The K_m for **3** in its reaction with HDAC1 was greater than 100 μM, although some curvature was observed in the rate vs [S] plot. Values of k_{cat}/K_m for HDAC1 and HDAC8 of 27000 and 50 M^{-1} s^{-1} were determined. These values are similar to those found for HDAC1 and HDAC8 in their reactions with **1**. These results suggest that the steric effects of the AMC moiety do not constitute a significant barrier to substrate binding to either HDAC as compared with naturally occurring amino acids.

Effect of Phosphorylation on HDAC1 Activity. It has been shown previously that HDAC1 is capable of being phosphorylated in vivo (*25*). The sites of phosphorylation were identified as serine residues 421 and 423 (*26*), and casein kinase II was shown to be capable of catalyzing the phosphorylation reactions (*25*, *26*). Whereas the phosphorylation of HDAC1 was shown to affect its incorporation into protein complexes, reactions of phosphorylated and nonphosphorylated HDAC1 with N-terminal histone H4 peptides showed either minor or negligible effects of phosphorylation on the catalytic activity of the HDAC1 enzyme (*25*, *27*).

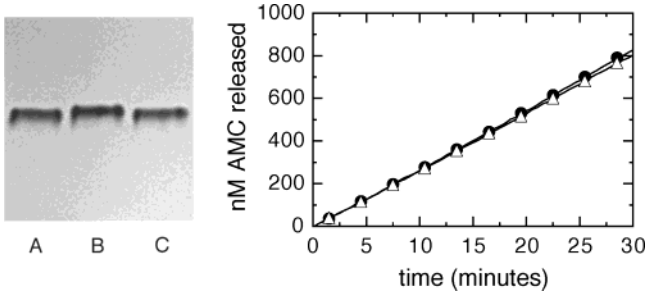

FIGURE 6: Reaction of HDAC1 with **1** as a function of HDAC1 phosphorylation state. HDAC1 was incubated for 2 h with casein kinase with or without added ATP. Aliquots were then removed for western blot analysis or activity measurements. Left: Western blot of HDAC samples. Lanes: A, untreated HDAC1; B, HDAC1 + casein kinase + ATP; C, HDAC1 + casein kinase, no ATP. Right: Progress curves for the reactions of treated HDAC1 with **1**. A lag time of 30 min was used to allow the reaction to reach steady state. The time point $t = 0$ is defined as the end of the lag time. Every sixth data point is denoted by a marker. Key: closed circles, HDAC1 + casein kinase + ATP; open triangles, HDAC1 + casein kinase, no ATP.

To assess directly whether the phosphorylation state of HDAC1 had an effect on the reaction kinetics of the enzyme with **1**, and as a comparison with literature reports, reactions of phosphorylated and nonphosphorylated HDAC1 with **1** were performed in parallel. The phosphorylation state of the isolated recombinant HDAC1 was established through treatment of HDAC1 with either placental alkaline phosphatase or casein kinase II, followed by gel mobility shift studies. This work revealed that, in our preparations of HDAC1, the enzyme was not phosphorylated as isolated. To test the relationship between HDAC1 phosphorylation and activity, a sample of HDAC1 was phosphorylated by the reaction with casein kinase II and ATP. In a control sample, HDAC1 was incubated with casein kinase II in the absence of ATP. Following a 2 h incubation, aliquots of the HDAC1 samples were subjected to gel electrophoresis and western blotting to verify the phosphorylation state of the enzyme. At the same time, additional aliquots of the two HDAC1 samples were used in the activity assay described above. The results of these experiments are shown in Figure 6. The left panel shows a western blot of untreated HDAC1 and the two treated HDAC1 samples. The sample treated with casein kinase and ATP (lane B) migrated more slowly than either untreated HDAC1 sample (lane A) or the sample treated with casein kinase and no ATP (lane C). This difference is consistent with phosphorylation of HDAC1 and agrees with gel shift data in the literature. The right panel in Figure 6 shows kinetic traces of the reactions of phosphorylated and nonphosphorylated HDAC1 with **1**. The rates were nearly identical for the two samples, differing by only 3%. Replicate studies showed this difference to be insignificant. These results demonstrate that the reaction of HDAC1 with **1** was not affected significantly by the phosphorylation state of the protein and thus that the immediate vicinity of the active site of the enzyme was not altered appreciably as a result of protein phosphorylation.

DISCUSSION

This study has provided a quantitative comparison of the reactivity of six HDAC enzymes. The kinetics served as a means of comparing both active site structure and reaction

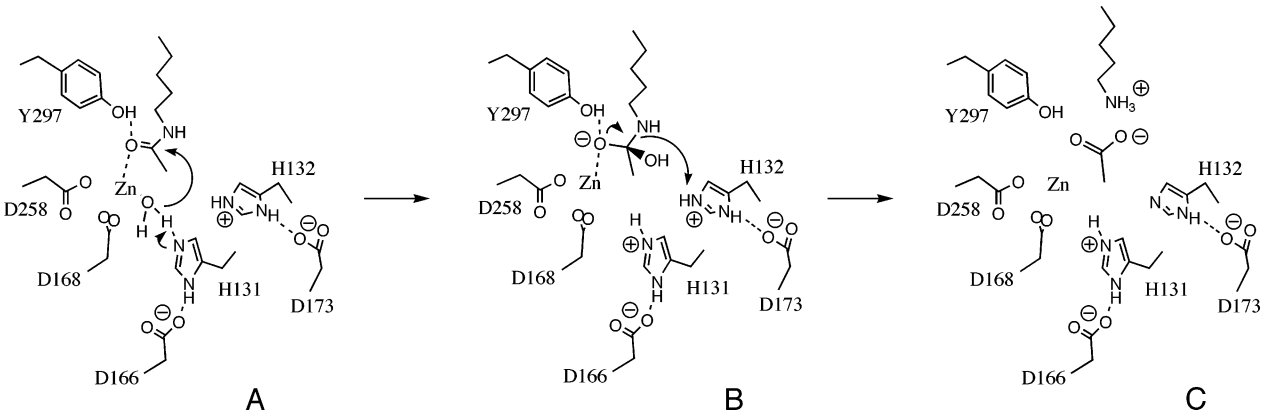

FIGURE 7: Proposed mechanism of the hydrolysis of acetyllysine by HDAC enzymes. This figure was adapted from ref *36*. Amino acid numbering is based on the HDLP protein sequence. The zinc ligand H170 is not shown for clarity.

mechanism among the isozymes. The study also allowed a determination of whether protein cofactors are required for activity and how they might modulate the catalytic activity of the HDAC enzymes. For five of the six HDAC enzymes studied, activity was observed from the isolated, recombinant proteins. This verified that other protein cofactors are generally not required for enzyme activity. Also, this precluded the possibility that the deacetylase activity assigned to a given isozyme may have arisen from copurification of a different HDAC isozyme, as has been observed in the study of class IIa HDAC enzymes (*28*).

The most prominent feature in the comparison of the kinetics of the HDAC enzymes in their reaction with **1** is the similarity of the kinetic parameters. HDAC1, HDAC2, and HDAC3/SMRT showed very similar rate constants, pH optima for the rate constants, and K_i values for inhibition by trichostatin A. This is in accord with the high sequence similarity between the isozymes (>55% identity, >70% homology) (*29*) and the conserved residues associated with the active site. HDAC6 showed similar parameters to HDACs 1, 2, and 3 despite a lower sequence similarity and different domain organization. However, in contrast to HDACs 1, 2, and 3, HDAC6 has been shown previously to be resistant to inhibition by aminoanilide-based inhibitors (*30*) and is also resistant to inhibition by trapoxin B (*31*) and butyrate (*32*).

The somewhat lower reaction rates observed with HDACs 8 and 10 suggest modest differences in active site structure from the other HDAC isozymes but are not likely to have a significant biological relevance on their own. The high K_m values observed in the reactions of HDAC8 with **1** and **3**, along with a K_i' value for TSA that was significantly higher for HDAC8 than for the other isozymes, suggest that the HDAC8 active site may be the most sterically hindered of the active sites probed in this work. In HDAC10, the catalytic domain is most similar to the N-terminal catalytic domain of HDAC6, but the sequence similarity is only 55% (*33*). Given the differences in the amino acid sequences between the two isozymes, a 100-fold difference in k_{cat} values between HDACs 6 and 10 is not unreasonable.

The presence of the SMRT peptide complexed with HDAC3 did not yield enzyme activity that was substantially different from the activities of the other HDAC isozymes. Previous reports have shown that HDAC3 requires the SMRT protein for activity and that chaperone proteins are required for the proper interaction of SMRT with HDAC3 (*13*, *34*, *35*). These observations imply that the association and dissociation of SMRT do not act as a readily reversible "switch" to modulate HDAC3 activity but that any disruption of the SMRT/HDAC3 interaction would simply cause the HDAC3 to denature. Similarly, the phosphorylation of HDAC1 has been shown to affect the binding of protein cofactors, but this work and the work of others (*25*, *27*) have shown that phosphorylation of HDAC1 does not affect the rate of reaction of HDAC1 with small substrates. Combined, these results suggest that the protein cofactors in the complete HDAC corepressor complexes do not switch the active sites from an inactive to an active conformation, or modulate the actual chemical transformation step in histone deacetylation, but rather that the cofactors serve to stabilize the HDAC enzymes, direct the enzymes to their biological targets, and contribute to substrate specificity.

Mechanistic Considerations. Structural information on the HDAC isozymes has come from the crystal structure determination of a histone deacetylase-like protein (HDLP) found in the thermophilic bacterium *Aquifex aeolicus* (*36*). The active site of this enzyme consists of a hydrophobic tunnel leading into the protein, at the bottom of which lies the catalytic core of the enzyme. The active site is shown schematically in Figure 7. The site of acetyllysine hydrolysis is a zinc atom coordinated by residues D168, D258, and H170 (HDLP numbering). Also in the active site are residues Y297, H131, and H132, all of which have been shown to be important for catalysis. Residues H131 and H132 are each hydrogen-bonded to aspartate residues (D166 and D173, respectively). On the basis of sequence alignments it appears that all of the residues listed above, along with the residues lining the hydrophobic tunnel, are conserved among the HDAC isozymes studied. Given the generally high sequence similarity between the isozymes, it is expected that the general mechanistic details of acetyllysine hydrolysis will likewise be similar for all isozymes.

On the basis of the crystal structure of the *A. aeolicus* enzyme, a reaction mechanism was proposed for acetyllysine hydrolysis by the family of HDAC enzymes. This mechanism is shown in Figure 7, using the HDLP amino acid numbering. In this scheme, acetyllysine binds at the active site through the interaction of the carbonyl oxygen atom with both the zinc atom and the phenolic hydrogen of Y297. These interactions polarize the C−O bond for nucleophilic attack. In addition, water binds to the zinc atom and forms a

hydrogen-bonding interaction with H131 that activates the water molecule (Figure 7A). The H131 residue deprotonates the water molecule, forming a hydroxide ion that can react with the carbonyl moiety of the acetyl group to form a tetrahedral intermediate (Figure 7B). This intermediate is stabilized by the interactions with the zinc ion and Y297. Finally, the intermediate collapses, forming acetate and free lysine. Protonated H132 serves as a general acid to protonate the lysine residue as it is deacetylated (Figure 7C) (*36*).

For the five HDAC isozymes in our study for which k_{cat} values were obtained, the pH dependencies were very similar. The pH profiles for all isozymes were bell-shaped with similar pH optima. This type of profile is expected for the proposed reaction mechanism. Groups in the active site that are likely to have pK_a values in this range include H131, H132, Y297, and zinc-bound water. Assignment of the pK_a values to specific residues is complicated by several features of the active site. Both H131 and H132 are involved in charge-relay interactions with aspartate residues, which are expected to increase the basicity of the histidines. Because there are multiple ionizable groups in the active site, the experimentally determined K_a values associated with the kinetic parameters will be molecular dissociation constants rather than dissociation constants for specific residues (*24*). Furthermore, because of the proximity of the active site residues, particularly H131 and H132, the ionization state of one group is likely to affect the pK_a of other residues. As a result of these issues, further studies will be necessary to assign pK_a values unambiguously and to provide a more conclusive demonstration of the reaction mechanism.

CONCLUSION

The kinetic studies described herein have yielded a quantitative comparison of the reactivity of six histone deacetylase isozymes and provide a basis for understanding the role of protein cofactors in the biological activity of the deacetylases. Of the six isozymes studied, HDACs 1, 2, 3, and 6 displayed very similar kinetics toward a small-molecule substrate, whereas HDACs 8 and 10 showed somewhat lower rates. The results imply that differentiation of the biological roles of the HDAC isozymes is likely to occur primarily on the basis of recruitment into corepressor complexes and on differential recognition of large protein substrates rather than on the intrinsic reactivity of individual isozymes. The observation of good hydrolytic activity of the isolated HDAC isozymes suggests that the protein cofactors of the HDAC isozymes are not necessary for enzyme activity but primarily serve to stabilize the protein and direct the enzyme to its biological targets.

The kinetics of the HDAC isozymes are consistent with the proposed mechanism of HDAC enzyme catalysis. A mechanism of zinc-mediated hydrolysis of acetyllysine residues assisted by general acid/base catalysis and transition-state stabilization is in accord with known mechanisms of metalloproteases (*37*). Our studies have yielded pH dependencies that are consistent with such a mechanism, and the assay methodology presented herein is readily applicable to a detailed mechanistic analysis of these enzymes. The biological role of the HDAC enzymes is an interplay of intrinsic reactivity of the HDAC enzyme and the biological strategies for compartmentalization, recruitment, and recognition of biological targets. With the kinetic parameters of the isolated HDAC enzymes serving as a baseline, the effect of the binding of protein cofactors on HDAC activity can now be explored further.

REFERENCES

1. Sterner, D. E., and Berger, S. L. (2000) Acetylation of histones and transcription-related factors, *Microbiol. Mol. Biol. Rev. 64*, 435−459.
2. De Ruijter, A. J. M., Van Gennip, A. H., Caron, H. N., Kemp, S., and Van Kuilenburg, A. B. P. (2003) Histone deacetylases (HDACs): characterization of the classical HDAC family, *Biochem. J. 370*, 737−749.
3. Verdin, E., Dequiedt, F., and Kasler, H. G. (2003) Class II histone deacetylases: versatile regulators, *Trends Genet. 19*, 286−293.
4. Blander, G., and Guarente, L. (2004) The Sir2 family of protein deacetylases, *Annu. Rev. Biochem. 73*, 417−435.
5. Knoepfler, P. S., and Eisenman, R. N. (1999) Sin meets NuRD and other tails of repression, *Cell 99*, 447−450.
6. Ng, H. H., and Bird, A. (2000) Histone deacetylases: silencers for hire, *Trends Biochem. Sci. 25*, 121−126.
7. Jepsen, K., and Rosenfeld, M. G. (2002) Biological roles and mechanistic actions of corepressor complexes, *J. Cell Sci. 115*, 689−698.
8. Seigneurin-Berny, D., Verdel, A., Curtet, S., Lemercier, C., Garin, J., Rousseaux, S., and Khochbin, S. (2001) Identification of components of the murine histone deacetylase 6 complex: link between acetylation and ubiquitination signaling pathways, *Mol. Cell. Biol. 21*, 8035−8044.
9. Hook, S. S., Orian, A., Cowley, S. M., and Eisenman, R. N. (2002) Histone deacetylase 6 binds polyubiquitin through its zinc finger (PAZ domain) and copurifies with deubiquitinating enzymes, *Proc. Natl. Acad. Sci. U.S.A. 99*, 13425−13430.
10. Durst, K. L., Lutterbach, B., Kummalue, T., Friedman, A. D., and Hiebert, S. W. (2003) The inv(16) fusion protein associates with corepressors via a smooth muscle myosin heavy-chain domain, *Mol. Cell. Biol. 23*, 607−619.
11. Kramer, O. H., Gottlicher, M., and Heinzel, T. (2001) Histone deacetylase as a therapeutic target, *Trends Endocrinol. Metab. 12*, 294−300.
12. Buggy, J. J., Sideris, M. L., Mak, P., Lorimer, D. D., McIntosh, B., and Clark, J. M. (2000) Cloning and characterization of a novel human histone deacetylase, HDAC8, *Biochem. J. 350*, 199−205.
13. Guenther, M. G., Barak, O., and Lazar, M. A. (2001) The SMRT and N-CoR corepressors are activating cofactors for histone deacetylase 3, *Mol. Cell. Biol. 21*, 6091−6101.
14. Jameson, G. W., Roberts, D. V., Adams, R. W., Kyle, W. S. A., and Elmore, D. T. (1973) Determination of the operational molarity of solutions of bovine α-chymotrypsin, trypsin, thrombin, and factor X*a* by spectrophotometric titration, *Biochem. J. 131*, 107−117.
15. Williams, J. W., and Morrison, J. F. (1979) The kinetics of reversible tight-binding inhibition, *Methods Enzymol. 63*, 437−467.
16. Wegener, D., Wirsching, F., Riester, D., and Schweinhorst, A. (2003) A fluorogenic histone deacetylase assay well suited for high-throughput activity screening, *Chem. Biol. 10*, 61−68.
17. Dai, Y., Guo, Y., Guo, J., Pease, L. J., Li, J., Marcotte, P. A., Glaser, K. B., Tapang, P., Albert, D. H., Richardson, P. L., Davidsen, S. K., and Michaelides, M. R. (2003) Indole amide hydroxamic acids as potent inhibitors of histone deacetylases, *Bioorg. Med. Chem. Lett. 13*, 1897−1901.
18. Inoue, A., and Fujimoto, D. (1970) Histone deacetylase from calf thymus, *Biochim. Biophys. Acta 220*, 307−316.
19. Hoffmann, K., Brosch, G., Loidl, P., and Jung, M. (1999) A nonisotopic assay for histone deacetylase activity, *Nucleic Acids Res. 27*, 2057−2058.
20. Grozinger, C. M., Hassig, C. A., and Schreiber, S. L. (1999) Three proteins define a class of human histone deacetylases related to yeast Hda1p, *Proc. Natl. Acad. Sci. U.S.A. 96*, 4868−4873.
21. Hubbert, C., Guardiola, A., Shao, R., Kawaguchi, Y., Ito, A., Nixon, A., Yoshida, M., Wang, X.-F., and Yao, T.-P. (2002) HDAC6 is a microtubule-associated deacetylase, *Nature 417*, 455−458.
22. Matsuyama, A., Shimazu, T., Sumida, Y., Saito, A., Yoshimatsu, Y., Seigneurin-Berny, D., Osada, H., Komatsu, Y., Nishino, N., Khochbin, S., Horinouchi, S., and Yoshida, M. (2002) In vivo

destabilization of dynamic microtubules by HDAC6-mediated deacetylation, *EMBO J. 21*, 6820−6831.
23. Haggarty, S. J., Koeller, K. M., Wong, J. C., Grozinger, C. M., and Schreiber, S. L. (2003) Domain-selective small-molecule inhibitor of histone deacetylase 6 (HDAC6)-mediated tubulin deacetylation, *Proc. Natl. Acad. Sci. U.S.A. 100*, 4389−4394.
24. Tipton, K. F., and Dixon, H. B. F. (1979) Effects of pH on enzymes, *Methods Enzymol. 63*, 183−234.
25. Cai, R., Kwon, P., Yan-Neale, Y., Sambuccetti, L., Fischer, D., and Cohen, D. (2001) Mammalian histone deacetylase 1 protein is posttranslationally modified by phosphorylation, *Biochem. Biophys. Res. Commun. 283*, 445−453.
26. Pflum, M. K., Tong, J. K., Lane, W. S., and Schreiber, S. L. (2001) Histone deacetylase 1 phosphorylation promotes enzymatic activity and complex formation, *J. Biol. Chem. 276*, 47733−47741.
27. Galasinski, S. C., Resing, K. A., Goodrich, J. A., and Ahn, N. G. (2002) Phosphatase inhibition leads to histone deacetylases 1 and 2 phosphorylation and disruption of corepressor interactions, *J. Biol. Chem. 277*, 19618−19626.
28. Fischle, W., Dequiedt, F., Hendzel, M. J., Guenther, M. G., Lazar, M. A., Voelter, W., and Verdin, E. (2002) Enzymatic activity associated with class II HDACs is dependent on a multiprotein complex containing HDAC3 and SMRT/N-CoR, *Mol. Cell 9*, 45−57.
29. Emiliani, S., Fischle, W., Van Lint, C., Al-Abed, Y., and Verdin, E. (1998) Characterization of a human RPD3 ortholog, HDAC3, *Proc. Natl. Acad. Sci. U.S.A. 95*, 2795−2800.
30. Wong, J. C., Hong, R., and Schreiber, S. L. (2003) Structural biasing elements for in-cell histone deacetylase paralog selectivity, *J. Am. Chem. Soc. 125*, 5586−5587.
31. Furumai, R., Komatsu, Y., Nishino, N., Khochbin, S., Yoshida, M., and Horinouchi, S. (2001) Potent histone deacetylase inhibitors built from trichostatin A and cyclic tetrapeptide antibiotics including trapoxin, *Proc. Natl. Acad. Sci. U.S.A. 98*, 87−92.
32. Guardiola, A. R., and Yao, T. P. (2002) Molecular cloning and characterization of a novel histone deacetylase HDAC10, *J. Biol. Chem. 277*, 3350−3356.
33. Fischer, D. D., Cai, R., Bhatia, U., Asselbergs, F. A. M., Song, C., Terry, R., Trogani, N., Widmer, R., Atadja, P., and Cohen, D. (2002) Isolation and characterization of a novel class II histone deacetylase, HDAC10, *J. Biol. Chem. 277*, 6656−6666.
34. Guenther, M. G., Yu, J., Kao, G. D., Yen, T. J., and Lazar, M. A. (2002) Assembly of the SMRT-histone deacetylase 3 repression complex requires the TCP-1 ring complex, *Genes Dev. 16*, 3130−3135.
35. Johnson, C. A., White, D. A., Lavender, J. S., O'Neill, L. P., and Turner, B. M. (2002) Human class I histone deacetylase complexes show enhanced catalytic activity in the presence of ATP and co-immunoprecipitate with the ATP-dependent chaperone protein Hsp70, *J. Biol. Chem. 277*, 9590−9597.
36. Finnin, M. S., Donigan, J. R., Cohen, A., Richon, V. M., Rifkind, R. A., Marks, P. A., Breslow, R., and Pavletich, N. P. (1999) Structures of a histone deacetylase homologue bound to the TSA and SAHA inhibitors, *Nature 401*, 188−193.
37. Lipscomb, W. N., and Sträter, N. (1996) Recent advances in zinc enzymology, *Chem. Rev. 96*, 2375−2433.

BI0494471